Targeting Norovirus Infection–Multivalent Entry Inhibitor Design Based on NMR Experiments

ARTICLE *in* CHEMISTRY - A EUROPEAN JOURNAL · JUNE 2011

Impact Factor: 5.73 · DOI: 10.1002/chem.201003432 · Source: PubMed

8 AUTHORS, INCLUDING:

Christoph Rademacher
Max Planck Institute of Colloids and Interfa…
30 PUBLICATIONS **434** CITATIONS
SEE PROFILE

Pavel I Kitov
University of Alberta
59 PUBLICATIONS **1,716** CITATIONS
SEE PROFILE

Brigitte Fiege
University of Basel
8 PUBLICATIONS **199** CITATIONS
SEE PROFILE

CHEMISTRY
A EUROPEAN JOURNAL

DOI: 10.1002/chem.201003432

Targeting Norovirus Infection—Multivalent Entry Inhibitor Design Based on NMR Experiments

Christoph Rademacher,[a, b] Julie Guiard,[c] Pavel I. Kitov,[c] Brigitte Fiege,[a] Kevin P. Dalton,[d] Francisco Parra,[d] David R. Bundle,[c] and Thomas Peters*[a]

Dedicated to Professor Heinz Rüterjans on the occasion of his 75th birthday

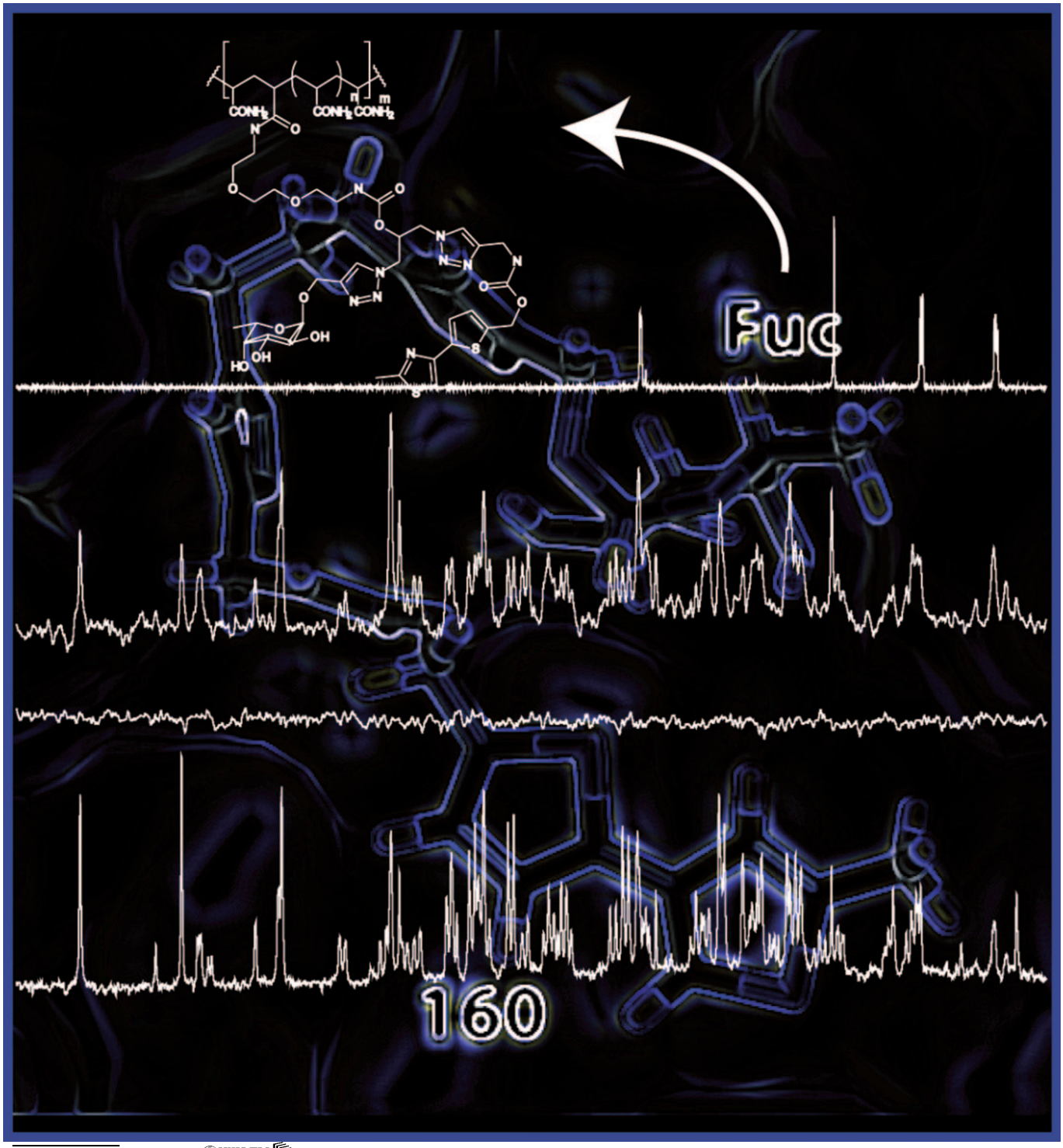

Abstract: Noroviruses attach to their host cells through histo blood group antigens (HBGAs), and compounds that interfere with this interaction are likely to be of therapeutic or diagnostic interest. It is shown that NMR binding studies can simultaneously identify and differentiate the site for binding HBGA ligands and complementary ligands from a large compound library, thereby facilitating the design of potent heterobifunctional ligands. Saturation transfer difference (STD) NMR experiments, spin-lock filtered NMR experiments, and interligand NOE (ILOE) experiments in the presence of virus-like particles (VLPs), identified compounds that bind to the HBGA binding site of human norovirus. Based on these data two multivalent prototype entry-inhibitors against norovirus infection were synthesized. A surface plasmon resonance based inhibition assay showed avidity gains of 1000 and one million fold over a millimolar univalent ligand. This suggests that further rational design of multivalent inhibitors based on our strategy will identify potent entry-inhibitors against norovirus infections.

Keywords: carbohydrates · entry inhibitor · NMR spectroscopy · norovirus · polymers · virology

Introduction

We explore here the concept that application of saturation transfer difference (STD) NMR[1] experiments in conjunction with other ligand-based NMR experiments can identify small molecules that bind to a known binding site on a virus surface, and to sites adjacent to the known binding site. Attachment of such ligands to a polymeric backbone yields multivalent inhibitors with enhanced avidity. Further optimization of such inhibitors may lead to potent polymeric inhibitors that will prevent viral entry into host cells.

In previous reports we have shown that STD NMR experiments significantly benefit from the large size of virus-like particles (VLPs).[2] In particular, saturation of protein signals is possible by setting the irradiation (on-resonance) frequency at values several ppm away from any ligand resonances, minimizing the chances of direct irradiation of ligand signals. STD NMR experiments have been used to identify and characterize the binding of ligands to native rhinoviruses,[2b] to rabbit hemorrhagic disease virus (RHDV) VLPs,[2a,3] to influenza virus VLPs,[4] and to bovine norovirus VLPs.[5] Experimental data show that epitope mapping of ligands binding to VLPs is feasible, although spin diffusion is significant for particles as large as VLPs. Practically, initial slopes of STD buildup curves deliver reliable and reproducible binding epitopes.[6] Along with other ligand-based NMR techniques, STD NMR[1] experiments are now being routinely used for ligand-based screening of protein targets (for reviews see reference [7]).

We have chosen to study human norovirus VLPs since noroviruses are responsible for epidemic outbreaks against which there is no known cure, nor effective vaccines. Structural data of norovirus VLPs,[8] or norovirus coat proteins complexed with ligands[9] are sparse, making structure-based design of entry inhibitors very difficult. Thus, the development of such inhibitors is a considerable challenge.

Noroviruses are a significant threat to human health[10] and belong to the family of *Caliciviridae* that comprises animal and human pathogens.[11] Caliciviruses cause a broad spectrum of acute or persistent infections, ranging from respiratory diseases, vesicular lesions, necrotizing hepatitis to diarrhea.[12] The viruses are non-enveloped and have an icosahedral shell constructed from a 60 kDa viral protein (VP1). For the study of virus-receptor recognition, virus-like particles (VLPs) are available that self-assemble from recombinant VP1 expressed in insect cells and that do not carry infectious viral RNA. VLPs are believed to have identical ligand-binding specificity as native virions.[13]

The *Norovirus* genus can be subdivided into five genogroups GI to GV, the human pathogens being included in GI, GII, and GIV.[14] The other two genogroups, GIII and GV, include strains from cows and mice. The murine strain, MNV-1, is the only norovirus that grows successfully in cell culture and in a small animal model.[15] Members of both GI and GII are major causes of epidemic outbreaks of non-bacterial gastroenteritis, with GII.4 being the most prominent agent of what is commonly referred to as "gastric flu".[16]

A cornerstone in the understanding of noroviral infections is the finding that histo blood group antigens (HBGA, Scheme 1, compounds **2**–**4b**) are essentially connected to the viral life cycle.[17] Studies of HBGA specificities for various members of the *Norovirus* genus based on data from agglutination and ELISA assays have been reviewed.[18]

Hemagglutination assays demonstrate that for GII.4 noroviruses, α-L-fucose, the common terminal monosaccharide of

[a] Dr. C. Rademacher, B. Fiege, Prof. Dr. T. Peters
Center of Structural and Cell Biology in Medicine
Institute of Chemistry, University of Luebeck
Ratzeburger Allee 160, 23562 Luebeck (Germany)
Fax: (+49) 451-500-4241
E-mail: thomas.peters@chemie.uni-luebeck.de

[b] Dr. C. Rademacher
Department of Chemical Physiology and Molecular Biology
The Scripps Research Institute, La Jolla, California (USA)

[c] Dr. J. Guiard, Dr. P. I. Kitov, Prof. Dr. D. R. Bundle
Department of Chemistry, University of Alberta
Edmonton, AB T6G 2G2 (Canada)

[d] Dr. K. P. Dalton, Prof. Dr. F. Parra
Instituto Universitario de Biotecnología de Asturias
Departamento de Bioquímica y Biología Molecular
Universidad de Oviedo, 33006 Oviedo (Spain)

Supporting information for this article is available on the WWW under http://dx.doi.org/10.1002/chem.201003432.

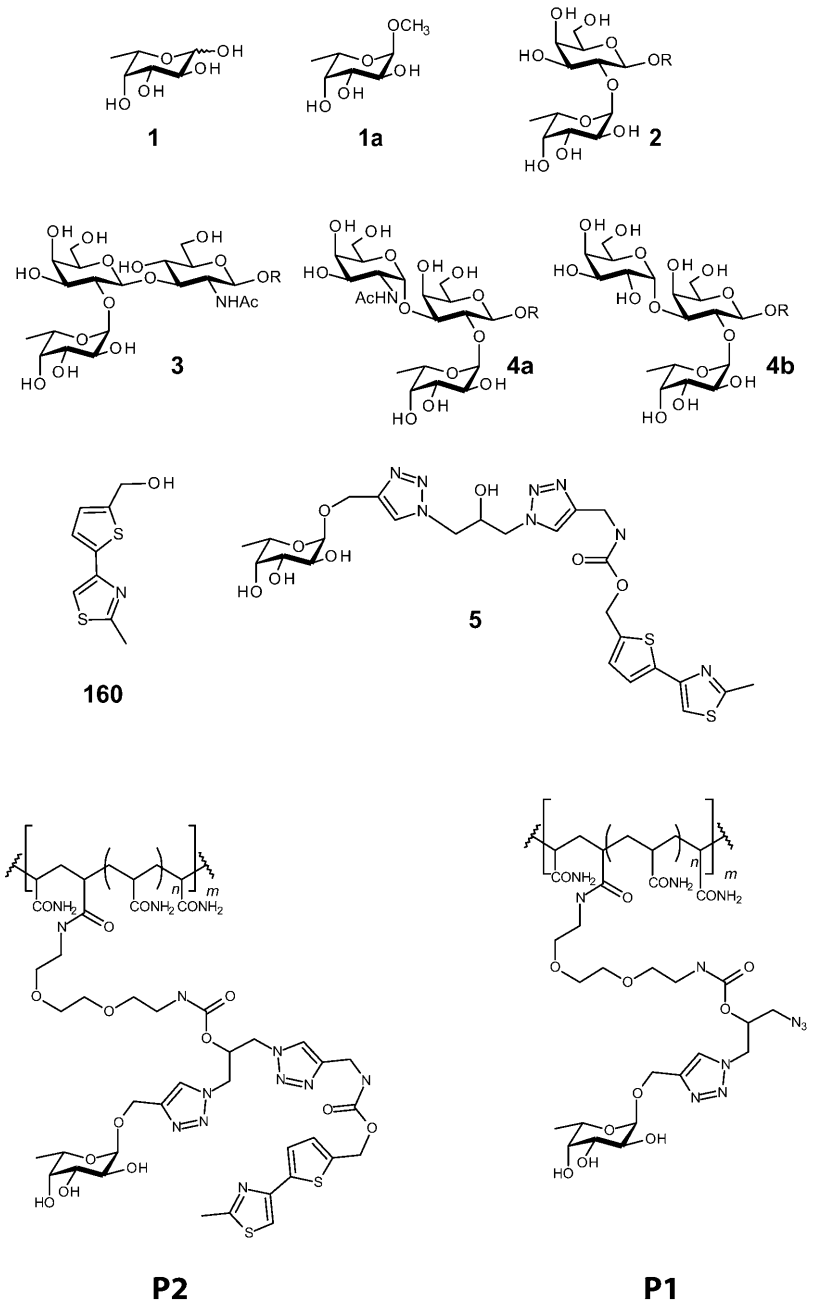

Scheme 1. L-Fucose (**1**), methyl-α-L-fucopyranoside (**1a**), H-disaccharide **2**, H-type I trisaccharide **3**, blood group A trisaccharide **4a**, and blood group B trisaccharide **4b**. R = octyl. Compound **160**, compound **5**, and the polymeric inhibitors **P1** and **P2** constructed from L-fucose (**1**) and compound **160**. Compound **5** is the monomeric unit of **P2**.

A, B, and H blood group antigens (Scheme 1, compounds **2**, **3**, **4a**, **4b**), is required for binding. We have shown by STD NMR spectroscopy that for the related rabbit hemorrhagic disease virus (RHDV) from the genus *Lagovirus*, α-L-fucose is the smallest fragment of the HBGA antigen with detectable binding to the viral coat. Similar results were obtained for the VLPs studied here.[19a]

Since crystallographic data on native caliciviruses or virus-like particles are only available for the virus without bound ligand,[8,19b] our understanding of receptor recognition originates from complexes of truncated capsid proteins, called P-dimers, with respective ligands. One structure of a P-dimer of the viral capsid of a GII.4 norovirus in complex with blood group A and B trisaccharides (Scheme 1, compounds **4a** and **4b**) has been solved.[9c] A first step towards an understanding of the evolutionary concept underlying HBGA recognition by noroviruses was made by Baric and co-workers, who found that the P2-domain evolves under positive selection in a linear fashion.[16b] Notably, multiple-sequence alignment of VP1 coat proteins of GII.4 norovirus strains that had occurred over the last 20 years shows that amino acid residues involved in L-fucose recognition are highly conserved.

Here we study for the first time the possibilities and perspectives of screening a commercially available small-compound library (Maybridge Ro5 500 Fragment Library, http://www.maybridge.com) for binding to norovirus (NV) VLPs[20] using STD NMR spectroscopy in conjunction with spin-lock filtering[21] experiments. Relaxation filtering such as spin-lock filtering for the detection of ligand binding was first proposed by Hajduk et al.[22] An interesting extension of this technique is the utilization of stable radicals as a source of efficient relaxation.[23] Our approach focuses on the α-L-fucose-binding subsite and its periphery, since the corresponding amino acids are highly conserved. In contrast to previous saliva-assay based screening of compound libraries,[24] this approach also provides structural information at atomic resolution on the ligand side.

Results and Discussion

The identification of small molecules with binding affinity for NV VLPs was subdivided into several steps. First,

ligand-based NMR screening of the Maybridge Ro5 library was performed by using a combination of STD NMR experiments and spin-lock filtered NMR spectra. This led to the identification of a rather large number of hits as both techniques can detect binding into the high millimolar range. Competitive STD NMR and spin-lock filtered NMR experiments identified those molecules that bind to the HBGA binding site. Competitive binding of hits was characterized in more detail using L-fucose (**1**), H-type I trisaccharide **3**, and blood group B-trisaccharide **4b** (Scheme 1) as inhibitors. The latter two steps yielded a much smaller set of compounds validated as competitive binders to the HBGA binding site. We then synthesized multivalent polymers by attaching α-L-fucose and alternatively α-L-fucose and one of the validated hits to a polyacrylamide backbone. The inhibition of binding of NV VLPs to immobilized H-antigen by these multivalent inhibitors was quantified by surface plasmon resonance experiments. Finally, we explored the possibility of binding sites adjacent to the fucose binding pocket by utilizing interligand NOE (ILOE) experiments.[25] The results of these experiments are presented in detail in the following.

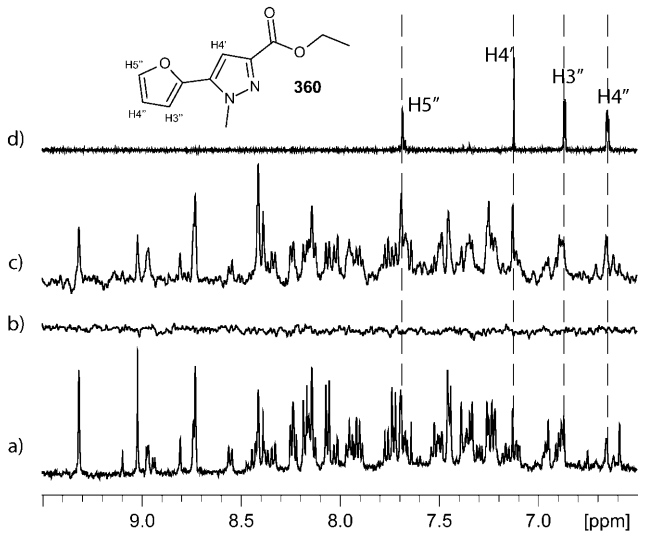

Figure 1. Screening of a mixture of 21 compounds with NMR spectroscopy. The expansions shown depict the region of aromatic protons. a) Reference ^{1}H NMR spectrum of the compound mixture in the presence of VLPs (22 nM). b), c) STD NMR spectra (256 scans, saturation time 4 s), in the absence (b) and in the presence (c) of VLPs. d) Reference ^{1}H NMR spectrum of compound **360** in the absence of VLPs. In all cases an exponential window function with a line broadening factor of 0.3 Hz has been applied. The spectra were recorded at 500 MHz at a temperature of 282 K. From a comparison of a) and c) it is obvious that the hit rate is very high.

Initial STD NMR screening of the Ro5 library: Only 86% of all compounds of the Maybridge library were soluble in water to the extent claimed by the supplier. Therefore, only 430 out of 500 compounds could be used for screening. Compound mixtures (bins) with an average of 30 compounds and a maximum number of 50 compounds in one mixture were prepared as described in the Experimental Section. In total, 14 bins were subjected to the NMR screening protocol. To exclude chemical reactions between fragments in a mixture, NMR spectroscopy was used to assure their integrity. A control experiment for one of the bins showed that the use of unique signals of individual components of the mixture might become critical if these signals give only weak STD effects. Only after removal of the hits from the bin and a repeated STD NMR experiment was an additional hit identified (cf. Figure S2 in the the Supporting Information).

Because of the excess of ligands over NV VLP binding sites of 10:1, assuming all 180 binding sites being intact, changes in chemical shifts or line broadening were usually not detectable. STD NMR spectra of compound mixtures in the presence of VLPs (a representative example is shown in Figure 1) immediately reveal a very high hit rate. Therefore, spin-lock filtered NMR experiments were performed with the same set of samples to validate the hits. The hits from spin-lock filter screening were identical with the ones from STD NMR screening.

Spin-lock filtering in the presence of VLPs: Spin-lock filtering reduces signal intensities of ligands binding to a protein receptor compared to signals of unbound ligands. Therefore, spin-lock filtering allows the detection of ligand binding.[22] Apparently, VLPs represent a very efficient source of T_2 relaxation and cause significant reduction of ligand signal intensities upon spin-lock filtering in the presence of VLPs. As an example, Figure 2 shows the aliphatic region of a bin consisting of 19 compounds. For instance, a signal reduction of about 80% is observed for the methyl group resonance signal of compound **231**.

Identification of fucose binding site ligands from competition STD NMR and spin-lock filtered NMR experiments: In a next step we performed competition STD NMR experiments to identify those ligands that bind to the fucose subsite of the HBGA binding site. Methyl α-L-fucopyranoside (**1a**) was added at approximately 15-fold molar excess to the mixtures from the initial screening, and a corresponding set of STD NMR spectra and spin-lock filtered NMR spectra was obtained. Competitive binding was detected by a reduction of STD effects or by a partial compensation of the attenuating effect of spin-lock filtering. Mixtures (bins) where no competition was observed were subjected to competition experiments with B-trisaccharide **4b** and H-type I trisaccharide **3** that bind to NV VLPs with higher affinity than methyl α-L-fucopyranoside (**1a**). An equimolar mixture of B-trisaccharide **4b** and H-type I trisaccharide **3** was added to the samples from the initial NMR screening, and again STD NMR and spin-lock filtered NMR spectra were recorded. This competitive screening left a total of 54 compounds (see Table S1 in the Supporting Information) that bind to the L-fucose subsite of the HBGA binding site, corresponding to a hit rate of 13%.

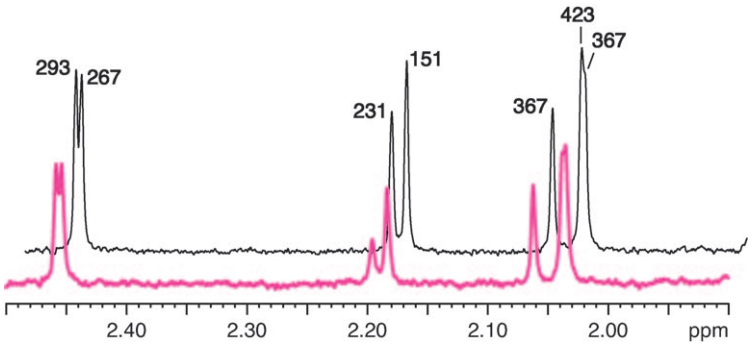

Figure 2. Comparison of spin-lock filtered (200 ms, 4 kHz) ^{1}H NMR spectra of a mixture of 19 compounds in the absence (black lines) and in the presence (magenta lines) of NV VLPs (22 nM). The ligand to VLP binding site ratio was about 10:1 for each component in the mixture. It was assumed that all 180 binding sites were intact. The spectral expansion shows the aliphatic region. For compound **231** a significant signal reduction of about 80% is observed upon spin-lock filtering in the presence of VLPs.

Binding activity of these compounds was further validated by spin-lock filtered NMR experiments and by STD NMR experiments with compound mixtures that contained only nine compounds each. Also, the concentration of NV VLPs was higher in these experiments than it had been in the initial screening (33 nM vs. 20 nM). Three compounds were identified as false positives and the remaining compounds were classified into categories according to the size of spin-lock mediated signal attenuations and STD effects (cf. Table S1 and Figure S3 in the Supporting Information). For the classification of compounds the reader is referred to the Experimental Section ("NMR screening protocol"). Only compounds from category 3 or 4 were subjected to a final validation step, where competition STD NMR experiments were performed as follows. The compounds were subjected to STD NMR experiments at a molar ratio of ligand to methyl α-L-fucopyranoside (**1a**) of 5:1. The C6 methyl group of **1a** served as a reporter STD signal that is attenuated in the presence of a competing ligand. All compounds from categories 3 and 4 attenuate the STD NMR signal of the C6 methyl group. Therefore, these experiments strongly support the binding data that are summarized in Table S1 in the Supporting Information. In total, the procedure furnished 26 compounds as validated fucose site binders corresponding to 6% of all compounds that bind to the L-fucose pocket of the HBGA binding site.

Synthesis of multivalent inhibitors: Based on the screening results and X-ray crystallographic studies we synthesized two prototype entry inhibitors. The crystal structure of the prototype Norwalk virus[8] reveals the general architecture of this class of viruses. The virus hull is composed of 180 VP1 proteins such that a maximum 180 HBGA antigens can bind to one virus. The VP1 proteins are arranged as dimers, and recent crystallographic studies on truncated so-called P-dimers expressed in *E.coli* and soaked with HBGA oligosaccharides have revealed that in the case of genogroup I noroviruses the binding sites are located on the monomeric units,[9a] whereas in the case of genogroup II noroviruses, to which the VLPs in this study belong, the HBGA binding site stretches across the dimer contact[9c] (cf. Figure S9 in the Supporting Information). In any case noroviruses exhibit an overall icosahedral symmetry. The distance between binding sites on a dimer is approximately 25 Å, and distances of approximately 75 Å are found to the next dimeric units (Figure 3). To obtain high avidity ligands we synthesized multivalent polymers (see accompanying paper of Guiard et al.[26]) that can position single fucose residues or compounds at distances found in the crystallographic study of Norwalk VLP.

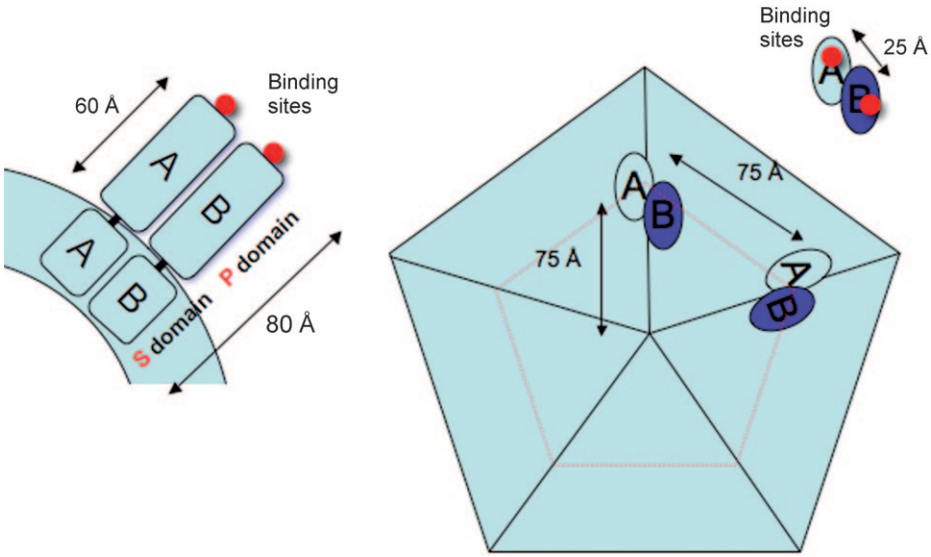

Figure 3. Cartoon showing the distribution of HBGA binding sites (red dots) on the viral surface. The drawing is based on the crystal structure of the prototype Norwalk virus[8] (pdb code: 1ihm). The relative location of binding sites is according to a crystallographic study of P-dimers soaked with B-trisaccharide[9a] (pdb code: 2obt). Left: Arrangement of VP1 proteins A and B on the surface of the icosahedrally shaped virus. Two monomeric VP1 proteins associate to generate AB dimers. The HBGA binding sites are located at the tips of the P-domains. Right: View down one of the fivefold symmetry axes of the VLP. HBGA binding sites are 25 Å apart on a dimer. The next AB dimer is found at a distance of 75 Å.

In a first example we have chosen a polyacrylamide backbone to which α-L-fucose is attached to yield inhibitor **P1** (Scheme 1). In **P1** one α-L-fucose is linked to every 30th propionylamide unit. The chain length of the polymers is approximately 1400 units. This design should allow simultaneous binding to HBGA binding pockets located on a dimer (25 Å) as well as to the next neighbors (75 Å). A second type of multivalent inhibitor has been obtained by simultaneously linking α-L-fucose, and in addition a compound from the pool of validated hits to the same propionylamide unit of the PAA backbone. We arbitrarily chose compound **160** to create inhibitor **P2** (Scheme 1). The synthesis of **P1** and **P2** and related polymers is described in an accompanying paper.[26]

Binding studies with surface plasmon resonance—Biacore-based binding assay: To obtain data on the binding affinity of HBGA ligands and to establish a binding assay that allows ranking of potential NV entry inhibitors, we performed surface plasmon resonance experiments. We applied a setup where an α-L-fucopyranoside linked to a polymeric backbone and labeled with biotin (α-L-fucopyranosyl-PAA-biotin) had been immobilized to a C1 chip through noncovalent neutravidin–biotin interactions.

A first set of experiments was performed to find the optimum pH for binding. A VLP solution of constant concentration was injected at different pH values and the amount of VLPs bound to the chip was measured after stopping the injection. Alternatively, VLP solution at pH 6.0 (MES buffer) was injected and washed off the chip with buffers at different pH. Both setups show that optimum binding is achieved around pH 6.0 (see Figure S5 in the Supporting Information).

In a second set of experiments the assay was used to determine IC_{50} values for the binding of L-fucose. As a control, competition experiments were also performed with D-galactose and D-glucose. For L-fucose an IC_{50} value of approximately 60 mM is found, whereas D-glucose and D-galactose do not interfere with binding of VLPs to the chip surface (see Figure S6 in the Supporting Information).

Finally, the binding avidity of polymers **P1** and **P2** was determined (Figure 4). In this case, determination of IC_{50} values was performed without subtracting the signal from the reference flow cell where only PAA–biotin had been immobilized on the chip surface due to a large proportion of unspecific binding of the VLPs to PAA–biotin. Presumably, the polymeric ligands not only block the specific binding to L-fucose residues exposed on the chip surface, but also hinder the whole surface of the VLPs from binding non-specifically. Therefore, the difference curves will reflect artifacts from blocking the unspecific interactions. When compared to L-fucose the IC_{50} value is reduced by a factor of about 10^3 for **P1** where only α-L-fucose is attached to the PAA backbone. For **P2**, where compound **160** and α-L-fucose are attached to the same propionylamide residues of the polymer, a reduction of the IC_{50} value by a factor of almost 10^6 is observed. The assay has also been used to measure the avidity

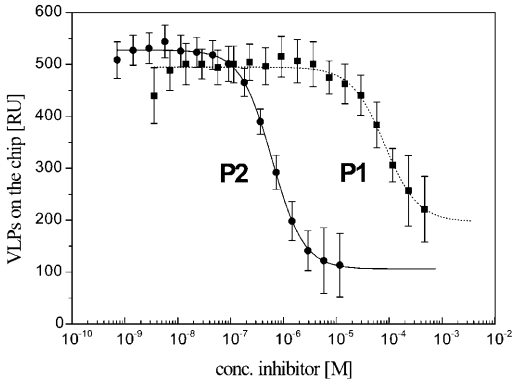

Figure 4. IC_{50} values of **P1** and **P2** as measured in a competitive surface plasmon resonance experiment. VLPs were pre-incubated with increasing concentrations of **P1** or **P2**, and the binding to multivalent α-L-fucopyranosyl-PAA-biotin immobilized to a neutravidin chip was measured as a function of inhibitor concentration: IC_{50}(**P2**) = 0.61 μM ±0.03 μM, IC_{50}(**P1**) = 80 μM ±30 μM. The inhibitor concentrations have been calculated from the molecular weights of L-fucose residues per polymer. It is estimated that the average polymer carries 20 L-fucose (**P1**) or 10 L-fucose and 10 compound **160** (**P2**) molecules. Based on this assumption **P1** contains 2842 g mol^{-1} L-fucose and **P2** 3160 g mol^{-1} L-fucose and compound **160**. It is clear that using the molecular weight of the polymers (60 to 100 kDa) one would arrive at much lower IC_{50} values in the pico- to nanomolar range.

of polymeric inhibitors related to **P1** and **P2** in reference [26]. All binding curves are shown in the Supporting Information of that paper and that study also includes data from a homogeneous assay based on STD NMR titrations that correlate well with the Biacore data.

Characterization of binding epitopes and bioactive conformations: For a qualitative epitope mapping of validated L-fucose site binders, STD NMR spectra were obtained for samples that contained methyl α-L-fucopyranoside (**1a**) from the titration experiments at a single saturation time of 1 s. A more reliable epitope mapping would require the acquisition of STD build-up curves to minimize effects of spin-diffusion and T_1 artifacts. Using a set of compounds where build-up curves and single saturation time experiments were compared, we estimate the systematic error introduced by performing single saturation time measurements to be 15% (see Figure S4 in the Supporting Information).

As compound **160** was used for the synthesis of a prototype polymeric entry-inhibitor **P2**, and since the heterobifunctional compound **5** that results from linking α-L-fucose through a spacer to compound **160** is the monomeric repeating unit of **P2**, a full binding epitope analysis was performed for compound **160** and for compound **5** (Figure 5). Unexpectedly, the carbamate linkage of compound **5** was observed to hydrolyze at neutral pH. The half-life of compound **5** and the corresponding polymeric version **P2** had a value of eleven days. This was sufficient to allow epitope analysis by STD NMR and Biacore inhibition assays.

For compound **160** we also acquired NOESY spectra in the presence of NV VLPs to detect transferred NOEs

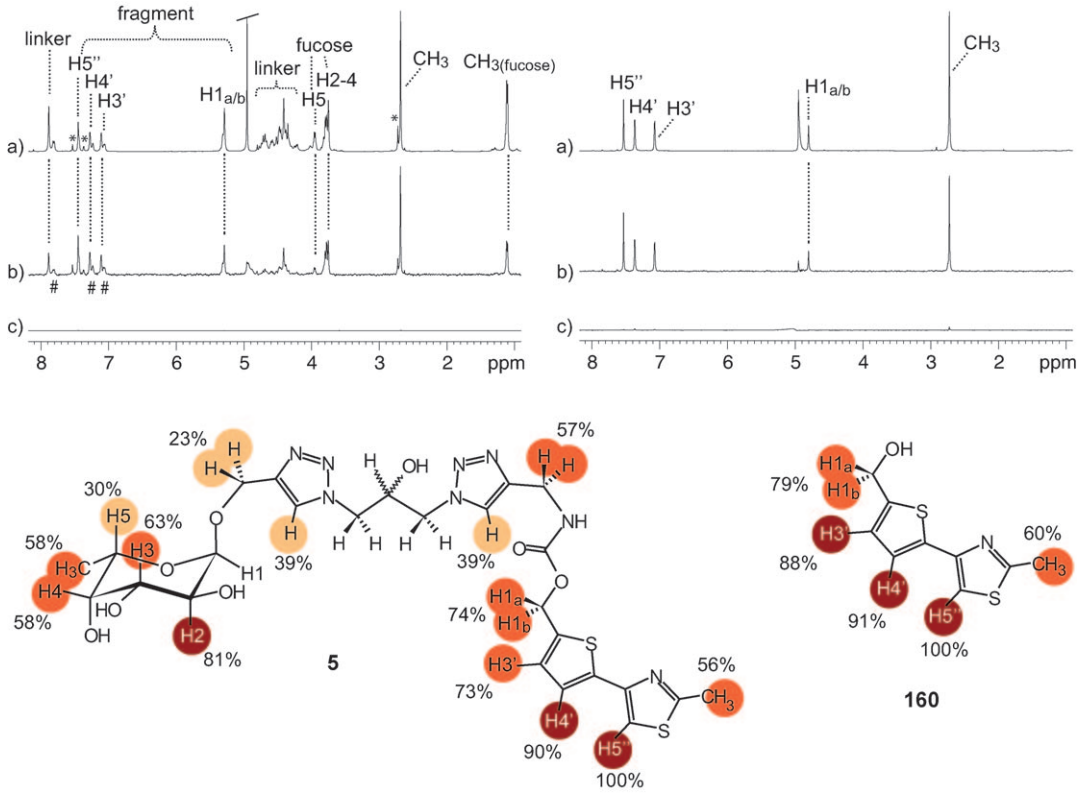

Figure 5. 500 MHz STD NMR spectra and binding epitopes for compounds **5** (left) and **160** (right) in the presence of NV VLPs. a) Reference ^{1}H NMR spectra and b) STD NMR spectra in the presence of NV VLPs. c) STD NMR spectra in the absence of NV VLPs. The on- and off-resonance frequencies were −4 ppm and 300 ppm, respectively. The spectra show that the carbamate linkage in **5** is not stable against hydrolysis because resonance signals of free **160** build up over time (labeled with asterisks in the left panel). The estimated half-life of **5** at a pH of 7.4 (D_2O) and a temperature of 282 K is 270 h. The appearance of a sharp and a broad peak (#) for each aromatic proton indicates micelle formation of **5**. The sharp peaks are left from the broad peaks. For H5″ the peaks overlap. The STD NMR spectrum of **5** shows almost no response from the linker region. Protons for which no STD percentage is given could not be treated quantitatively because of signal overlap or due to the water suppression.

(trNOEs) for the analysis of the bioactive conformation of **160** bound to NV VLPs. Transferred NOEs were identical with NOEs of **160** in the absence of NV VLPs, showing that the bioactive conformation of **160** is identical with the prevalent conformation in aqueous solution (Figure S8). The bioactive conformation of **160** is largely defined by a distance restraint due to a NOE/trNOE between protons H5′ and H4. The binding epitopes of **5** and **160** and the bioactive conformation of **160** are used to identify docking models (Figure 6) that are in accordance with the NMR experiments as discussed below.

Identification of adjacent site ligands using interligand NOEs (ILOEs): ILOEs are powerful tools to identify ligands binding to an adjacent site. Here, we were interested in the identification of ligands that bind adjacent to the fucose binding site. Therefore, we performed NOESY experiments for mixtures of compounds in the presence of methyl α-L-fucopyranoside (**1a**). In a control experiment, we first tested ligands from categories 3 and 4 that were pooled into two respective bins. NOESY spectra in the presence of NV VLPs showed trNOEs but as expected no ILOEs were observed, neither for any pair of fragments, nor with **1a**. This supports the results from competitive STD NMR experiments that had identified these compounds as fucose binding site ligands.

Then, compounds that bind to NV VLPs but that had been ruled out as fucose binding site ligands were subjected to NOESY experiments in the presence of **1a**. Fifty compounds were selected based on the size of their STD and spin-lock filter effects and divided into four bins that were subjected to NOESY experiments in the presence of NV VLPs and **1a**. These experiments yielded ILOEs between **1a** and four compounds **151**, **191**, **231**, and **473** (see Figure S7 in the Supporting Information). Control NOESY experiments in the absence of NV VLPs showed no ILOEs. For validation, each of the four compounds was subjected to a NOESY experiment in the presence of NV VLPs and **1a**. These single compound experiments confirmed that **151**, **191**, **231**, and **473** bind to a site that is adjacent to the fucose binding site.

Discussion

Human milk protects infants against norovirus infection most likely due to the presence of glycan chains, which may have a high affinity for attaching to norovirus surfaces and thus preventing infection. Whereas saliva screening assays of this activity may be fast they lack important information about structural aspects of binding.[24] In contrast, the structure of binding epitopes and their bioactive conformation can be revealed by STD NMR and transferred NOESY experiments. We have shown that such ligand-based NMR analysis, and in particular STD NMR studies of virus–ligand or VLP–ligand interactions benefit significantly from the large size of viruses or VLPs.[2a] For example, on-resonance saturation frequencies can be set at frequency values far away from any ligand resonance lines and direct irradiation artifacts are avoided. This creates possibilities for ligand-based NMR screening of compound libraries for binding activity to intact viruses or VLP hulls. In the case of noroviruses the minimal unit that recognizes HBGA antigens on host cells is a dimer, the so-called P-dimer,[27] but it is uncertain how well receptor recognition of norovirus VLPs is reflected by norovirus P-dimers.[27,28] Consequently, VLPs are more representative of the binding properties of native noroviruses.

Here, we describe the first application of ligand-based NMR screening to identify compounds with virus-binding activity from a fragment library. The hits from this screening served as fragments for the design of multivalent antiviral entry inhibitors using norovirus Ast6139/01/Sp VLPs as an example target. We screened 430 compounds of the Ro5 500 Maybridge library to identify ligands that bind to the fucose-binding pocket of the HBGA binding site, or to adjacent or overlapping binding pockets. To arrive at validated hits we employed 1.5 mg NV VLP (600 μg of VLPs were used for the initial screening of 15 bins), and less than 200 μg of each ligand. In particular, it was not necessary to deconvolute mixtures as long as spectral overlap allowed unambiguous identification of all members of a bin. With a total instrument time of approximately 170 h (not counting the time required for the acquisition of reference NMR spectra for the individual compounds and not including the NMR experiments for spectra assignments) our study demonstrates that ligand-based NMR screening of VLPs or whole viruses is a practical approach.

It is well documented that ligand-based NMR screening allows identification of low affinity binders, and thus "non-specific" binding may obscure the analysis of data.[29] In the case of VLPs as target, substantially higher hit-rates are observed than reported before for smaller protein targets[29,30] because the sensitivity of the NMR readout is much higher in the case of very large protein targets (VLPs). Also, we have chosen the experimental conditions for STD NMR experiments such that identification of hits is "safe" even in mixtures with severe signal overlap. A saturation time of 4 s is associated with significant spin diffusion amongst protons of ligands that bind, thus allowing the use of single resonance lines for the identification of binding ligands in complex mixtures. In order not to miss any hits we also set no arbitrary threshold for the size of STDs to mark a compound as hit.

Not surprisingly the initial screening of NV VLPs with the Maybridge library led to a hit rate of 61%. At first sight this high rate may seem unfavorable especially in comparison to, for example, a study where FABP4 (MW 14.7 kDa) had been screened with a 532-member fragment library yielding an overall hit rate of only 10%.[29] A set of subsequent NMR experiments substantially narrowed the compounds of interest for viral entry inhibitors. The experiments done were a) competition NMR experiments and b) ILOE experiments. Competition STD NMR experiments in conjunction with spin-lock filtered competition experiments yielded a subset of 13% of compounds that have binding affinity for the HBGA binding pocket. More elaborate STD NMR titrations, in which the suppression of the STD signal of the C6 methyl group of L-fucose was monitored, left only 26 compounds out of 430 as competitive binders corresponding to a hit rate of 6% with respect to L-fucose site binders (cf. Table S1 in the Supporting Information). This is well within the range of hit-rates in previous studies targeting isolated proteins but not whole viruses or VLPs.

For the design of novel multivalent NV entry-inhibitors we assumed that a multivalent inhibitor would effectively mimic the host-cell surface and thus would lead to ligands with enhanced binding avidity. In recent years concepts of multivalency[31] have proven to be extremely successful for the design of potent inhibitors, for example, against Shiga toxin.[31e] In the case of norovirus infection there have been recent attempts to synthesize hydrogels that present B-trisaccharide as a decoy to prevent infection.[32] Second, we asked the question whether it is possible to devise potent multivalent inhibitors based on the minimal recognition element for NV VLPs, namely α-L-fucose. Third, we considered that potent multivalent inhibitors could be based on small molecules that had been identified to inhibit binding of α-L-fucose to norovirus VLPs.

To test these hypotheses we synthesized one polyacrylamide-based multivalent inhibitor **P1** that carried only α-L-fucose residues and another polymer **P2** that carried α-L-fucose and compound **160**, identified as a L-fucose-binding inhibitor as described above.[26] From crystallographic data we have identified two main distances of 25 or 75 Å between HBGA binding sites (cf. Figure 3). Therefore, attachment of the α-L-fucose residues or compound **160** to every 30th propionyl residue should create a polymer that simultaneously binds to several fucose-binding pockets on the VLP surface.

The avidities of the prototype polymeric inhibitors **P1** and **P2** were determined by using surface plasmon resonance experiments (Biacore, Figure 4). Compared to the data for monomeric L-fucose (Figure 5), polymeric presentation as in **P1** improves the binding avidity by a factor of about 10^3. The attachment of a competitive binder (compound **160**) as in **P2** improves the binding avidity by another three orders

of magnitude. In **P2**, α-L-fucose and compound **160** are attached to the PAA backbone through flexible linkers allowing maximum distances between the two ligands of less than approximately 20 Å. This arrangement does not allow simultaneous binding to two adjacent HBGA sites on one dimer (cf. Figure 3). To explain the increase in binding avidity of **P2** versus **P1** we propose the existence of additional binding pockets to which fucose or compound **160** can bind. To validate this hypothesis we synthesized compound **5**, which constitutes the monomeric unit of **P2**, and subjected **5** to NMR experiments and docking studies.

The binding mode of prototype NV entry inhibitors was derived from NMR experiments and docking studies. To analyze the binding mode of the polymeric inhibitor **P2** we obtained binding epitopes from STD NMR experiments (cf. Figure 5) for the constituent compounds **160** ([5-(2-methylthiazol-4-yl)-2-thienyl]methanol) and **5**. From the binding epitope of compound **5** it is seen that L-fucose and compound **160** are the pharmacophoric groups that make close contact to the viral surface. For compound **160** preliminary data from transferred NOESY experiments (cf. see Figure S8 in the Supporting Information) suggest that protons H4′ and H5″ are in close proximity when bound to the viral coat. This would restrict rotation around the C4′–C5″ bond. Docking experiments were performed by using compound **5** as a ligand and using the crystal structure of P-dimers of VA387[9c] (pdb code: 2obt) as a target. Construction of a homology model of Ast6139/01/Sp was not necessary since VA387 and Ast6139/01/Sp have 96% sequence identity (cf. Figure S10 in the Supporting Information). The docking was performed by employing the Vina protocol.[33]

Interestingly, the highest predicted affinity when docking the fucose monosaccharide to VP1 was obtained for a docking mode in which fucose was placed in the position found for the fucose moiety of the B-trisaccharide in the crystal structure.[9c] However, since Autodock Vina found at least nine putative bound poses within an affinity range of 0.5 kcal mol^{-1}, all of them should be regarded as equipotential (considering that the standard error of affinity scoring in Vina is 2.75 kcal mol^{-1}). Another site most frequently visited by the fucose probe is formed by Ser 441, Ala346, Lys348, Asp374, His347, the site occupied by α-Gal in the crystal structure. Interestingly, this second site is preferred by the fucose moiety when docking compound **5** into VP1 (see Figure 6). In the pose shown, the fucose moiety occupies this second putative binding site while the thiazole moiety of **5** overlaps with the fucose position found in the crystal structure supporting the observation that fucose and **160** compete for the same binding site on the protein surface. This pose agrees well with the experimental binding epitope of compound **5** from STD NMR experiments (Figure 5): H-4′ and H-5″ of the **160** moiety are in direct contact with the protein, whereas methyl and methylene groups are solvent exposed. For the fucose moiety, H-2, H-3, H-4, and one proton of the C-6 methyl group are in close contact with the protein surface, whereas H-5 is solvent exposed. In agreement with this, H-5 experiences the lowest amount of saturation transfer (Figure 5). The aromatic protons in both triazole rings as well as the methylene group linked to the anomeric oxygen of fucose are rather remote from the protein surface in agreement with the experimental STD NMR data. Finally, the conformation of the glycosidic bond is in accord with the *exo*-anomeric effect.

Thus, the model of compound **5** bound to VP1 presented in Figure 6 is experimentally validated and will serve as a working hypothesis for future inhibitor design.

It is interesting to put these results into perspective with recent crystallographic studies[18,19] on genogroup I (Norwalk) P-dimers soaked with H-pentasaccharide[18] (cf. H-trisaccharide **3** in Scheme 1, which represents the non-reducing end of the H-pentasaccharide) or with A-trisaccharide **4a** (Scheme 1).[19] Compared to the fucose-binding pocket of genogroup II noroviruses, that is, in the structure of VA387[20] complexed with B-trisaccharide **4b**, the L-fucose binding pocket is about 13 Å away. Moreover, one of these studies[18] shows that the binding mode of A-trisaccharide is different from the one for the H-pentasaccharide. In the case of the A-trisaccharide the *N*-acetyl group of the GalNAc residue takes the place of the α-L-fucose moiety of the H-pentasaccharide. To illustrate this, we have mapped the HBGA binding site of Norwalk virus onto the structure

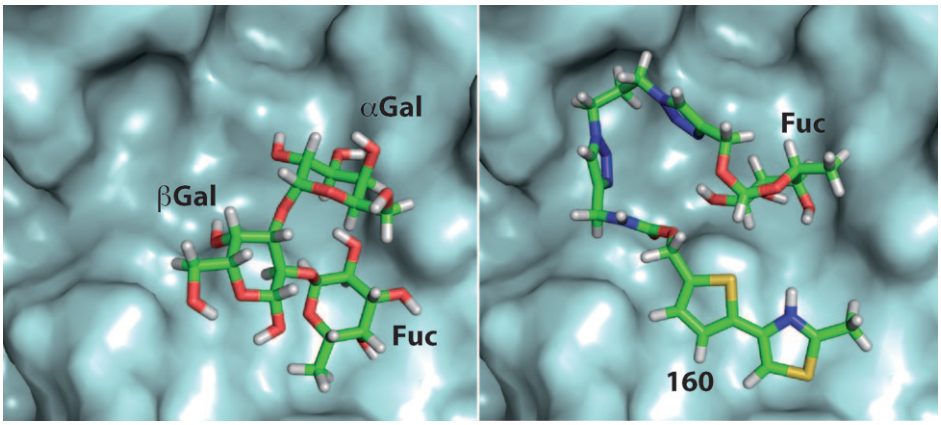

Figure 6. Right: Docking model of **5** in the HBGA-binding pocket of norovirus VLPs. This docking model has been selected on the basis of NMR experimental restraints (trNOEs and STD effects) from a number of possible poses derived from AutoDock Vina as described in the text. Left: For the docking study the crystal structure of P-dimers of VA387 VLPs soaked with B-antigen trisaccharide was used (pdb code: 2obt). The picture was prepared using PyMOL (http://www.delanoscientific.com/). The comparison between the crystal structure (left) and the docking model shows that **160** as part of **5** occupies the L-fucose binding pocket. This is in excellent agreement with competition STD NMR experiments.

of VA387 in Figure S9 in the Supporting Information. Although the amino acids involved in HBGA binding are not conserved across genogroups I (Norwalk) and II (VA387) the data highlight a change of the position of the fucose-binding site with evolution. This is indirect support for our hypothesis of secondary fucose-binding pockets on the surface of noroviruses.

Finally, we asked whether it is possible to identify small compounds that bind to sites adjacent to the fucose binding pocket. STD NMR experiments had defined a subset of compounds that showed binding affinity but that did not bind to the fucose pocket of the HBGA binding site and had been discarded for the synthesis of multivalent inhibitors. We subjected this subset of compounds to ILOE experiments that identify compounds binding to sites that are close enough to allow the observation of NOEs between protons of the ligands occupying the two adjacent sites (proton–proton distances of less than ca. 5 Å are required). These experiments identified four compounds **151**, **231**, **191**, and **473** (cf. Figure S7 in the Supporting Information) that showed ILOEs to protons of methyl α-L-fucopyranoside (**1a**), and therefore are assumed to bind to a binding pocket adjacent to the fucose pocket. Such compounds are valuable building blocks that may be chemically linked to α-L-fucose to generate more potent inhibitors.

It is of interest to note that none of the compounds identified in the present screen have shown up as hits when the Maybridge library was screened against the human blood group B galactosyltransferase (GTB)[34] as target protein. Thus the two sets of hits are orthogonal adding credibility to the target specificity of the screening protocol.

Conclusion

We have shown that it is possible to design entry inhibitors against norovirus infection using mainly STD and NOE-based NMR experiments with whole virus-like particles instead of isolated coat protein. This approach is beneficial because the arrangement of coat proteins in the virus hull can create binding pockets that are not present in isolated or truncated coat proteins. The synthesis of two prototype polymeric inhibitors proves that this approach can indeed deliver high avidity binders.

As a perspective, ILOE data suggest that the four fragments **151**, **191**, **231**, and **473** could be linked to α-L-fucose to deliver monomeric ligands with increased binding affinities that in turn could be used as building blocks for the synthesis of multivalent inhibitors. We are currently pursuing this approach to obtain more potent inhibitors of norovirus infections.

Experimental Section

Fragment library handling: The Maybridge Ro5 500 Fragment Library (2006) was purchased from Thermo Fisher Scientific Inc. The compounds were delivered in pure form as powder or liquid. All compounds were dissolved in 25 mM phosphate buffer (pH* 7.0) in D_2O to yield a final concentration of 2 mM. Compounds with a computed solubility below 2 mM were dissolved to yield a final concentration of 1 mM. Computed solubilities were provided by Thermo Fisher Scientific Inc. After buffer addition, the compounds were shaken for 1 h at 37 °C. The solubility was verified visually. When particles or aggregates were observed, samples were shaken at room temperature overnight. In some cases compounds were placed in an ultrasound water bath at room temperature for 5 min, followed by rigorous shaking. Stock solutions were stored at −20 °C. ^{1}H NMR spectra of all soluble compounds in buffer were recorded at a concentration of 1 mM in the presence of 0.4 mM TSP as reference.

The assignment of ^{1}H chemical shifts was performed by using standard 1D and 2D NMR methods. In many cases 1D chemical shift selective filtered (cssf) NOESY or ROESY or both yielded sufficient information to assign the resonances.[35] Data were compared to information from a ^{1}H chemical shift prediction server, namely SPINUS WEB[36] and the NMRShiftDB (http://nmrshiftdb.ice.mpg.de/). The Spectral Database for Organic Compounds (SDBSWeb: http://riodb01.ibase.aist.go.jp/sdbs/ (National Institute of Advanced Industrial Science and Technology, 2008)) was also used.

Design of compound mixtures: A python script (available upon request from the authors) was written to provide compound mixtures (bins) based on the following rules: 1. No chemical reaction between the members of a bin is allowed. To fulfill this requirement, SMILES code filtering rules were used according to Hann et al.[37] to identify acids, bases, nucleophiles, and electrophiles (for SMILES definitions see the Supporting Information). 2. At least one unique ^{1}H NMR resonance line per compound must be available for the identification in a mixture. A separation of at least 0.01 ppm of this resonance line from any other resonances was considered sufficient. 3. Only compounds with the same number of rotatable bonds were permitted in one bin. If that renders the bin size too small, only minor differences are allowed between members of the same bin.

NMR screening protocol: The compound mixtures had a maximum total concentration of organic molecules of less than about 2.0 mM. Therefore, each ligand was present at a concentration of 40 μM. The screening of a compound mixture was performed in five steps:

1. Acquisition of a ^{1}H NMR spectrum of each compound mixture and comparison to spectra from single molecules to ensure that no chemical reaction has occurred.

2. Acquisition of STD NMR spectra in the absence of VLPs under the same conditions as in the presence of VLPs. 256 Scans were recorded for on- and off-resonance experiments at a saturation time of 4.0 s, a relaxation delay of 1.0 s, and an acquisition time of 2.7 s, resulting in a total delay between two on-resonance scans of 11.4 s. The on-resonance frequency was set at −4 ppm and the off-resonance frequency was 300 ppm.[2a] The pulse train for saturation consists of repeats of 49 ms Gaussian-shaped pulses at 50 dB attenuation and a 1 ms inter pulse delay. The saturation power of a single Gaussian pulse was 63 Hz. Finally, a ^{1}H NMR spectrum with a 200 ms continuous wave spin-lock filter (3.96 kHz) was employed with 128 scans and 8 dummy scans at a carrier frequency of 4.7 ppm.

3. VLP stock solution was titrated into the solution of compound mixture to yield a final VLP concentration of 22 nM. The same set of ^{1}H NMR, spin-lock-filtered ^{1}H NMR and STD NMR experiments as described above was acquired. The STD experiments were performed with twice the number of scans.

4. Methyl α-L-fucopyranoside (**1a**) was added resulting in a 15-fold excess over a single compound to the mixtures. STD NMR experiments were recorded under the same conditions as described above.

5. Addition of an equimolar mixture of B-antigen trisaccharide **4b** and H-antigen trisaccharide (type I) **3** to the mixtures. Then, the NMR experiments were repeated as described in 2.

STD NMR experiments: STD NMR experiments were recorded following the protocol reported before.[2a] To find optimum conditions for STD screening the S/N ratio was monitored as a function of relaxation delay

and saturation time for a given STD signal of a bin with 50 compounds (cf. Figure S1 in the Supporting Information). A repetition time of approximately 11 s, comprising acquisition time, relaxation delay, and saturation time, between two on-resonance experiments was optimal. This value was used throughout this study and led to good S/N ratios of up to 10:1 in STD NMR spectra within about one hour of experimental time.

Criteria for hit selection: STD and spin-lock-filtered ^{1}H NMR spectra were analyzed by employing a 3 Hz line broadening and zero filling to 64 k data points. If the saturation transfer to a particular compound was reduced by addition of both methyl α-L-fucopyranoside and the trisaccharide mixture, the compound was considered as a hit for the α-L-fucose binding site. If reduction only took place during the second titration step the compound was assigned to the pool of potential B-antigen trisaccharide or H-antigen trisaccharide (type I) binders. Compounds binding to VLPs were identified by inspection of STD NMR and spin-lock filtered spectra.

Compounds that were identified as specific ligands for the α-L-fucose binding site of Ast6139 VLPs from competition experiments were pooled into six bins. These mixtures contained equal concentrations of each ligand (200 μM) and VLPs (33 nM) present. Fucose binding site specificity was validated by addition of α/β-L-fucose **1** (Sigma) in a 105:1 excess and the reduction of saturation transfer as well as the reduction of signal intensity due to application of a spin-lock filter was recorded. STD NMR spectra were acquired under the same conditions as stated above except for the number of scans (128 scans were used for on- and off-resonance experiment, respectively). Compounds were assigned to one of four categories defined as follows: Category 1: False positives, that is, compounds that show no STD or do not compete with L-fucose for binding; Category 2: reduction of signal intensity due to spin-lock filtering is less than 10% or a small STD effect (<10%) combined with low spin-lock suppression (<20%); Category 3: strong signal reduction greater than 40% upon application of a spin-lock filter; Category 4: compounds with a large STD amplification factor (>10%) but with signal reduction due to spin-lock filtering less than 40%.

Compounds assigned to categories 3 and 4 were subjected to a final validation step reversing the order of titration. Samples containing methyl α-L-fucopyranoside (200 μM) and VLPs (11 nM) were titrated with the respective ligand (1 mM). Careful preparation of the stock solutions ensured equal conditions for all ligands. Data were evaluated based on the reduction of the STD effect of the methyl α-L-fucopyranoside H6 proton (δ ^{1}H = 1.24 ppm). STD NMR spectra were recorded including the following changes (vide supra): 1.0 s saturation time, a prescan delay of 1.0 s and 256 scans for on- and off-resonance, respectively. NOESY spectra were recorded with a mixture of each category in order to detect potential interligand NOEs (ILOEs)[25] between ligands. Spectra were recorded with 64 scans, a mixing time of 800 ms, a relaxation delay of 1.5 s, 4096 complex data points in the direct and 256 complex data points in the indirect dimension.

Biacore experiments

SPR analysis of Ast6139 VLPs with prototype inhibitors: SPR experiments were performed on a BIAcore 3000 instrument (GE Healthcare). C1 sensor chips (Biacore) were covered with Neutravidine using the standard Amine Coupling Kit (Biacore). PAA-biotin as well as multivalent α-L-fucopyranosyl-PAA-biotin obtained from Glycotech were diluted to 1 to 10 μg mL^{-1} in HBS-P (Biacore) and immobilized on the chip (90 to 175 RU). The running buffer for the following experiments was 50 mM MES buffer pH 6 with 154 mM NaCl, 0.01% NaN_3 and 0.005% surfactant. For all experiments a single batch of 3 μg μL^{-1} Ast6139 VLPs in 20 mM PBS pH 7.2 was used.

Determination of IC_{50} values of L-fucose: α/β-L-Fuc (**1**) (Sigma), α/β-D-Gal (Fluka) and α/β-D-Glc (Merck) were dissolved in MES buffer (pH 6.0), respectively, to yield a final concentration of 400 mM. These solutions of α/β-D-Gal, α/β-D-Glc and α/β-L-Fuc were diluted 1:1 in the running buffer five times ($\log_2$-dilution series). α/β-L-Fuc (**1**) was diluted another five times. First, at a flow rate of 25 μL min^{-1} 25 μL of 25 μg mL^{-1} VLPs in MES (pH 6.0) were injected. The injection was followed by the EXTRACLEAN procedure to ensure that the needle is clean before the next injection. The stationary phase of the resulting sensorgram was then used to monitor the competition between the monosaccharides and the immobilized α-L-fucopyranosyl-PAA-biotin. Regeneration was started after 5.5 min. Series of α/β-D-Gal and α/β-D-Glc injections were separated by cleaning the instrument using the PRIME command. A competition series of ten 1:1 dilutions of α/β-L-Fuc was measured against four additional 1:1 dilutions of the VLPs. Data were fitted with a non-linear least squares algorithm written in Scientific Python to the Hill equation (1):

$$RU(c_{lig}) = RU_{mim} + \frac{RU_{\max} - RU_{\min}}{1 + 10^{(\log(IC_{50}) - \log(c_{lig}))Hillslope}} \quad (1)$$

with RU_{min} and RU_{max} being the minimum and the maximum RU measured, $LogIC_{50}$ being the logarithm of the IC_{50} value and *HillSlope* being the Hill coefficient.

Competition assay with multivalent inhibitors: In a competition based assay format VLPs were preincubated with varying concentrations of inhibitors for 2 h in MES buffer pH 6. Binding of VLPs to the immobilized PAA-glycans was monitored at a flow rate of 5 μL min^{-1}. The average response units (RU) at the end of the injection phase in the difference curves as a function of inhibitor concentration were used to derive IC_{50} values. Regeneration of the chip surface was achieved by injection of 1 M NaCl in 50 mM NaOH. Inhibitors **P1** and **P2** were synthesized as described below. Response curves were analyzed with BIAEvalutation software (Biacore) and Origin 7.0 (Microcal).

Acknowledgements

T.P. thanks the Deutsche Forschungsgemeinschaft (DFG) for a grant Pe494/8–1 and for grants HBFG 101/192–1 and ME 1830/1. C.R. thanks the Verband der Chemischen Industrie (VCI) for a stipend and B.F. thanks the Studienstiftung des deutschen Volkes for a stipend. Work at F. Parra's laboratory has been supported by grant BIO2009–07535 from the Spanish Ministerio de Ciencia e Innovación and the European Union FEDER program. D.R.B. is a recipient of a Humboldt Research Award. Financial support for J.G., P.I.K., and D.R.B. was provided by Alberta Ingenuity Centre for Carbohydrate Science and the Natural Science and Engineering Research Council of Canada.

[1] M. Mayer, B. Meyer, *Angew. Chem.* **1999**, *111*, 1902–1906; *Angew. Chem. Int. Ed.* **1999**, *38*, 1784–1788.
[2] a) C. Rademacher, N. R. Krishna, M. Palcic, F. Parra, T. Peters, *J. Am. Chem. Soc.* **2008**, *130*, 3669–3675; b) A. J. Benie, R. Moser, E. Bauml, D. Blaas, T. Peters, *J. Am. Chem. Soc.* **2003**, *125*, 14–15.
[3] A. O. Frank, H. Kessler, *Nature* **2008**, *452*, 822–823.
[4] T. Haselhorst, J. M. Garcia, T. Islam, J. C. Lai, F. J. Rose, J. M. Nicholls, J. S. Peiris, M. von Itzstein, *Angew. Chem.* **2008**, *120*, 1936–1938; *Angew. Chem. Int. Ed.* **2008**, *47*, 1910–1912.
[5] M. Zakhour, N. Ruvoen-Clouet, A. Charpilienne, B. Langpap, D. Poncet, T. Peters, N. Bovin, J. Le Pendu, *PLoS Pathog.* **2009**, *5*, e1000504.
[6] C. Rademacher, T. Peters, *Top. Curr. Chem.* **2008**, *273*, 183–202.
[7] a) C. Ludwig, U. L. Guenther, *Front. Biosci.* **2009**, *14*, 4565–4574; b) E. R. Zartler, H. Mo, *Curr. Top Med. Chem.* **2007**, *7*, 1592–1599; c) B. Meyer, T. Peters, *Angew. Chem.* **2003**, *115*, 890–918; *Angew. Chem. Int. Ed.* **2003**, *42*, 864–890; d) M. Coles, M. Heller, H. Kessler, *Drug Discovery Today* **2003**, *8*, 803–810; e) D. F. Wyss, M. A. McCoy, M. M. Senior, *Curr. Opin. Drug Discov. Devel.* **2002**, *5*, 630–647; f) B. J. Stockman, C. Dalvit, *Prog. Nucl. Magn. Reson. Spectrosc.* **2002**, *41*, 187–231; g) S. Rudisser, W. Jahnke, *Comb. Chem. High Throughput Screening* **2002**, *5*, 591–603; h) D. S. Sem, M. Pellecchia, *Curr. Opin. Drug Discov. Devel.* **2001**, *4*, 479–492; i) T. Diercks, M. Coles, H. Kessler, *Curr. Opin. Chem. Biol.* **2001**, *5*, 285–291; j) C. A. Lepre, J. M. Moore, J. W. Peng, *Chem. Rev.* **2004**, *104*, 3641–3676.

[8] B. V. Prasad, M. E. Hardy, T. Dokland, J. Bella, M. G. Rossmann, M. K. Estes, *Science* **1999**, *286*, 287–290.
[9] a) J. M. Choi, A. M. Hutson, M. K. Estes, B. V. Prasad, *Proc. Natl. Acad. Sci. USA* **2008**, *105*, 9175–9180; b) W. Bu, A. Mamedova, M. Tan, M. Xia, X. Jiang, R. S. Hegde, *J. Virol.* **2008**, *82*, 5340–5347; c) S. Cao, Z. Lou, M. Tan, Y. Chen, Y. Liu, Z. Zhang, X. C. Zhang, X. Jiang, X. Li, Z. Rao, *J. Virol.* **2007**, *81*, 5949–5957.
[10] M. Koopmans, *Curr. Opin. Infect. Dis.* **2008**, *21*, 544–552.
[11] K. Y. Green, T. Ando, M. S. Balayan, T. Berke, I. N. Clarke, M. K. Estes, D. O. Matson, S. Nakata, J. D. Neill, M. J. Studdert, H. J. Thiel, *J. Infect. Dis.* **2000**, *181 Suppl 2*, S322–330.
[12] H. J. Thiel, M. Konig, *Vet. Microbiol.* **1999**, *69*, 55–62.
[13] a) A. D. Hale, D. C. Lewis, X. Jiang, D. W. Brown, *J. Med. Virol.* **1998**, *54*, 305–312; b) X. Jiang, D. O. Matson, G. M. Ruiz-Palacios, J. Hu, J. Treanor, L. K. Pickering, *J. Clin. Microbiol.* **1995**, *33*, 1452–1455; c) K. Y. Green, J. F. Lew, X. Jiang, A. Z. Kapikian, M. K. Estes, *J. Clin. Microbiol.* **1993**, *31*, 2185–2191; d) X. Jiang, M. Wang, D. Y. Graham, M. K. Estes, *J. Virol.* **1992**, *66*, 6527–6532.
[14] D. P. Zheng, T. Ando, R. L. Fankhauser, R. S. Beard, R. I. Glass, S. S. Monroe, *Virology* **2006**, *346*, 312–323.
[15] C. E. Wobus, L. B. Thackray, H. W. t. Virgin, *J. Virol.* **2006**, *80*, 5104–5112.
[16] a) B. Lopman, M. Zambon, D. W. Brown, *PLoS Med.* **2008**, *5*, e42; b) L. C. Lindesmith, E. F. Donaldson, A. D. Lobue, J. L. Cannon, D. P. Zheng, J. Vinje, R. S. Baric, *PLoS Med.* **2008**, *5*, e31.
[17] a) A. M. Hutson, R. L. Atmar, D. M. Marcus, M. K. Estes, *J. Virol.* **2003**, *77*, 405–415; b) P. Huang, T. Farkas, S. Marionneau, W. Zhong, N. Ruvoen-Clouet, A. L. Morrow, M. Altaye, L. K. Pickering, D. S. Newburg, J. LePendu, X. Jiang, *J. Infect. Dis.* **2003**, *188*, 19–31; c) S. Marionneau, N. Ruvoen, B. Le Moullac-Vaidye, M. Clement, A. Cailleau-Thomas, G. Ruiz-Palacois, P. Huang, X. Jiang, J. Le Pendu, *Gastroenterology* **2002**, *122*, 1967–1977; d) P. R. Harrington, L. Lindesmith, B. Yount, C. L. Moe, R. S. Baric, *J. Virol.* **2002**, *76*, 12335–12343.
[18] a) M. Tan, X. Jiang, *Curr. Opin. Investig. Drugs* **2008**, *9*, 146–151; b) M. Tan, X. Jiang, *Expert Rev. Mol. Med.* **2007**, *9*, 1–22; c) M. K. Estes, B. V. Prasad, R. L. Atmar, *Curr. Opin. Infect. Dis.* **2006**, *19*, 467–474; d) M. Tan, X. Jiang, *Trends Microbiol.* **2005**, *13*, 285–293.
[19] a) B. Fiege, C. Rademacher, P. I. Kitov, F. Parra, M. M. Palcic, T. Peters, unpublished results; b) R. Chen, J. D. Neill, M. K. Estes, B. V. Prasad, *Proc. Natl. Acad. Sci. USA* **2006**, *103*, 8048–8053.
[20] J. A. Boga, S. Melon, I. Nicieza, I. De Diego, M. Villar, F. Parra, M. De Ona, *J. Clin. Microbiol.* **2004**, *42*, 2668–2674.
[21] T. Scherf, J. Anglister, *Biophys. J.* **1993**, *64*, 754–761.
[22] J. H. Hajduk, E. T. Olejniczak, S. W. Fesik, *J. Am. Chem. Soc.* **1997**, *119*, 12257–12261.
[23] a) W. Jahnke, S. Rudisser, M. Zurini, *J. Am. Chem. Soc.* **2001**, *123*, 3149–3150; b) W. Jahnke, M. J. Blommers, C. Fernandez, C. Zwingelstein, R. Amstutz, *ChemBioChem* **2005**, *6*, 1607–1610.
[24] X. Feng, X. Jiang, *Antimicrob. Agents Chemother.* **2007**, *51*, 324–331.
[25] R. E. London, *J Magn Reson* **1999**, *141*, 301–311.
[26] J. Guiard, B. Fiege, P. I. Kitov, T. Peters, D. R. Bundle, *Chem. Eur. J.* **2011**, *17*, DOI: 10.1002/chem.201003414.
[27] M. Tan, R. S. Hegde, X. Jiang, *J. Virol.* **2004**, *78*, 6233–6242.
[28] M. Tan, W. Zhong, D. Song, S. Thornton, X. Jiang, *J. Med. Virol.* **2004**, *74*, 641–649.
[29] N. Baurin, F. Aboul-Ela, X. Barril, B. Davis, M. Drysdale, B. Dymock, H. Finch, C. Fromont, C. Richardson, H. Simmonite, R. E. Hubbard, *J. Chem. Inf. Comput. Sci.* **2004**, *44*, 2157–2166.
[30] M. J. van Dongen, J. Uppenberg, S. Svensson, T. Lundback, T. Akerud, M. Wikstrom, J. Schultz, *J. Am. Chem. Soc.* **2002**, *124*, 11874–11880.
[31] a) D. R. Bundle, *Nat. Chem. Biol.* **2007**, *3*, 605–606; b) N. Horan, L. Yan, H. Isobe, G. M. Whitesides, D. Kahne, *Proc. Natl. Acad. Sci. USA* **1999**, *96*, 11782–11786; c) P. I. Kitov, D. R. Bundle, *J. Am. Chem. Soc.* **2003**, *125*, 16271–16284; d) P. I. Kitov, T. Lipinski, E. Paszkiewicz, D. Solomon, J. M. Sadowska, G. A. Grant, G. L. Mulvey, E. N. Kitova, J. S. Klassen, G. D. Armstrong, D. R. Bundle, *Angew. Chem.* **2008**, *120*, 684–688; *Angew. Chem. Int. Ed.* **2008**, *47*, 672–676; e) P. I. Kitov, J. M. Sadowska, G. Mulvey, G. D. Armstrong, H. Ling, N. S. Pannu, R. J. Read, D. R. Bundle, *Nature* **2000**, *403*, 669–672.
[32] Y. Zhang, Q. Yao, C. Xia, X. Jiang, P. G. Wang, *ChemMedChem* **2006**, *1*, 1361–1366.
[33] O. Trott, A. J. Olson, *J. Comput. Chem.* **2009**, *30*, 455–461.
[34] C. Rademacher, J. Landstrom, N. Sindhuwinata, M. M. Palcic, G. Widmalm, T. Peters, *Glycoconjugate J.* **2010**, *27*, 349–358.
[35] P. T. Robinson, T. N. Pham, D. Uhrin, *J. Magn. Reson.* **2004**, *170*, 97–103.
[36] J. Aires-de-Sousa, M. C. Hemmer, J. Gasteiger, *Anal. Chem.* **2002**, *74*, 80–90.
[37] M. Hann, B. Hudson, X. Lewell, R. Lifely, L. Miller, N. Ramsden, *J. Chem. Inf. Comput. Sci.* **1999**, *39*, 897–902.

Received: November 27, 2010
Published online: May 12, 2011

